


RESEARCH ARTICLE

 View Article Online
View Journal | View Issue

 Cite this: *Mater. Chem. Front.*,
2023, 7, 2839

Hole-transport-layer-free CdSe/ZnS core/shell red quantum-dot light-emitting diodes sensitized by TADF polymers†

 Yuhan Gao,^{ab} Qin Xue^{*c} and Guohua Xie  ^{*ab}

Due to high photoluminescence quantum yields, narrow bandwidths and tunable colors, quantum dot light emitting diodes (QLEDs) have become one of the most promising display technologies. To simplify the device structure and improve the charge transport, a thermally activated delayed fluorescence (TADF) polymer was introduced into the emitting layer as an assistant host in this work. The TADF polymer facilitates the efficient utilization of triplet excitons through reverse intersystem crossing, promoting Förster energy transfer to QDs. By optimizing the host selection, the emission from the TADF polymer itself could be suppressed, which significantly improved the color purity of QLEDs. Without using any hole transport layer, the fabricated CdZnS/ZnS core/shell red QLEDs showed a maximum external quantum efficiency of 18.1%. The cascaded energy transfer in the ternary emitting layer provides a promising strategy to construct highly efficient and simplified QLEDs.

 Received 7th February 2023,
Accepted 4th April 2023

DOI: 10.1039/d3qm00130j

rsc.li/frontiers-materials

Introduction

Quantum dots (QDs) possess excellent luminescent properties, such as narrow emission line-widths, tunable emission, and high photoluminescence quantum yield (PLQY).^{1–4} The core/shell QDs are one of the most promising candidates for improving the stability of quantum-dot light emitting diodes (QLEDs).^{5,6} In most QLED architectures, metal oxide ZnO is widely used as the electron transporting layer (ETL), given its efficient electron mobility ($\sim 10^{-3} \text{ cm}^2 \text{ V}^{-1} \text{ s}^{-1}$) and well aligned energy levels.⁷ However, the imbalanced charge injection caused by excess electrons could lead to unwanted Auger recombination, and the high annealing temperature of ZnO might damage the QD layer during the fabrication of QLEDs with a non-inverted device architecture.⁸ To overcome these problems, many researchers focused on modifying the hole transporting layer (HTL), *e.g.*, the multilayered HTLs,⁹ and the composition of metal oxides to balance charge injection. Nevertheless, there are still a lot of challenges due to the complex structure of QLEDs and sensitive nature of metal oxide to the

environment and preparation procedures. To this end, organic semiconducting materials would be good substitutes of metal oxide-based ETLs in QLEDs.¹

Besides the ETLs, the HTL and the emitting layer also play important roles in determining device performance. For QLEDs, poly(*N,N'*-bis(4-butylphenyl)*N,N'*-bis(phenyl)benzidine) (poly-TPD),¹⁰ poly(*N*-vinylcarbazole) (PVK),¹¹ and poly[bis(4-phenyl)(2,4,6-trimethylphenyl)amine] (PTAA),¹² have been commonly used as HTLs. However, the increasing thickness of the HTL based devices may deteriorate hole transport due to the low mobility. In addition, it is challenging to screen appropriate orthogonal solvents for HTLs once QDs are dissolved in a particular solvent, *e.g.*, toluene.¹³ To address this issue, the use of HTL-free structures would be a good option to simplify the fabrication procedure. However, the HTL-free architecture would risk charge injection and lead to inferior electroluminescence performance. Moreover, for HTL-free devices, the optimization of the EMLs is necessary. In organic light emitting diodes (OLEDs), a host:guest codoped system is commonly used to suppress the concentration quenching of the emitter and promote energy transfer from the host to the guest.^{14,15} Recently, thermally activated delayed fluorescence (TADF) materials have attracted great attention due to their high external quantum efficiencies (EQEs), surpassing the limit of traditional fluorescent OLEDs.^{15–17} Meanwhile, the efficient and bipolar charge transport make them very good candidates as hosts.

Our group has demonstrated that a TADF:QDs host-guest system can greatly improve the efficiencies of red QLEDs,

^a The Institute of Flexible Electronics (Future Technologies), Xiamen University, Xiamen 361005, China. E-mail: ifeghxie@xmu.edu.cn

^b Sawage Center for Molecular Sciences, Hubei Key Lab on Organic and Polymeric Optoelectronic Materials, Department of Chemistry, Wuhan University, Wuhan, 430072, China. E-mail: guohua.xie@whu.edu.cn

^c Department of Physical Science and Technology, Central China Normal University, Wuhan 430079, China. E-mail: xueqin@mail.ccnu.edu.cn

† Electronic supplementary information (ESI) available. See DOI: <https://doi.org/10.1039/d3qm00130j>

obtaining a maximum EQE of 11.8%.¹⁸ Nevertheless, the host 10,10'-(sulfonylbis(4,1-phenylene))bis(2,7-bis(3,6-di-*tert*-butyl-9H-carbazol-9-yl)-9,9-dimethyl-9,10-dihydroacridine)(4CzDMAC-DPS) itself has residual emission in the doped QLED, leading to low color purity.

Encouraged by the previous work, the orange TADF polymer PCzAQCO.5 was chosen as an assistant sensitizer to construct a doped EML.¹⁹ This conjugated polymer possesses excellent TADF properties with a high PLQY of 80% and a small singlet–triplet gap (ΔE_{ST}). Moreover, it has excellent film forming properties which are mandatory for solution-processed devices. Herein, we demonstrated a HTL-free simple structure and highly efficient CdZnSe/CdZnS-ZnS core/shell red QLEDs. Based on the binary EML of PCzAQCO.5:QD, the HTL-free device realized a maximum EQE of 12.4%, which is over 2-fold higher than that (6.1%) of the device with the commonly used host PTAA. To further suppress the residual emission of PCzAQCO.5, we screened the host 1,3-bis(carbazol-9-yl) benzene (mCP) to construct a ternary-blended EML, *i.e.*, a host:TADF sensitizer:QD system. Finally, HTL-free red QLEDs with a high color purity of 97.0% were obtained. After further optimization, a maximum EQE of 18.1% (29.2 cd A⁻¹ and 20.4 lm W⁻¹) was achieved. To the best of our knowledge, this is the highest EQE of red QLEDs with organic ETLs. We believe this new strategy will be universal and contribute to the development of simplified and highly efficient QLEDs.

Results and discussion

As shown in Fig. 1a, the red QD film has a narrow full-width at half-maxima (FWHM) with a sharp photoluminescence (PL) spectrum peak at 620 nm. The PL spectrum of the TADF polymer PCzAQCO.5 displays a good overlap with the absorption spectrum of the QD film, which is beneficial for facilitating energy transfer. The chemical structures of the organic materials used in the EMLs involved in this investigation are shown in Fig. S1 (ESI[†]). To construct efficient HTL-free QLEDs, we measured and compared the fluorescence quenching effect of QDs on different substrates. The neat glass, the modified hole injecting material poly(3,4-ethylenedioxythiophene):poly(styrene sulfonate) (m-PEDOT:PSS),²⁰ and the commonly used hole transporting material poly[bis(4-phenyl)(2,4,6-trimethylphenyl)amine] (PTAA) were respectively chosen as substrates for depositing the QD films. As shown in Fig. 1b, the steady PL spectra of glass/QD showed the highest intensity,

which indicated that either energy transfer or fluorescence quenching happened when PTAA and m-PEDOT:PSS were inserted, respectively. Apparently, the PTAA/QD film suffered severe fluorescence loss. Nevertheless, the PL intensity of m-PEDOT:PSS/QD film remained slightly higher than that of the PTAA/QD film, indicating a reduced non-radiative recombination.

The transient PL lifetimes of QDs on these three substrates (see Fig. 1c) also proved the above conclusion. The glass/QD film showed the longest lifetime (18.7 ns) among the three samples. In contrast, the lifetimes of the PTAA/QD and m-PEDOT:PSS/QD films were 11.0 and 12.5 ns, respectively. All the results clearly showed that the modified interface can reduce exciton loss, making it feasible to construct more efficient HTL-free devices.

Since the electroluminescence (EL) performance of QLEDs does not simply depend on the photophysical properties, we fabricated three devices to exemplify the HTL-free strategy. Following the device structures of indium tin oxide (ITO)/m-PEDOT:PSS (50 nm)/EML (40 nm)/bis[2-(diphenylphosphino)phenyl]ether oxide (DPEPO) (10 nm)/1,3,5-tri(m-pyrid-3-yl-phenyl)benzene (TmPyPB) (50 nm)/lithium 8-hydroxyquinolinolate (Liq) (1 nm)/Al (100 nm), and ITO/m-PEDOT:PSS (50 nm)/PTAA (20 nm)/EML (40 nm)/DPEPO (10 nm)/TmPyPB (50 nm)/Liq (1 nm)/Al (100 nm) as references, we compared the device performances with and without the HTL. Due to the mismatched energy levels and thus a huge charge injecting barrier, the device with the HTL based on the neat QD layer was not working. As shown in Table S1 (ESI[†]), we introduced a conjugated polymer PCzAQCO.5 as a host to dilute QDs to promote energy transfer and energy level alignment. The TADF polymer PCzAQCO.5 is easily soluble in organic solvent and possesses excellent film forming properties. Due to its small ΔE_{ST} to realize efficient reverse intersystem crossing (RISC), the film is highly emissive.

The EL characteristics of QLEDs are presented in Fig. 2 and Table S1 (ESI[†]). The EML was composed of PCzAQCO.5:(20 wt.%) QDs. The distinctive luminance–voltage–current density curves shown in Fig. 2a indicated that the HTL-free device exhibited the lower driving voltage at high brightness over 100 cd m⁻², mainly due to the well-matched energy levels. With increasing driving voltage, the HTL with PTAA tended to dissipate voltage due to high resistance. Moreover, the maximum EQE of the HTL-free device with the binary-blended EML reached 12.4%. In contrast, the PTAA based device exhibited an inferior EQE of 6.1% (see Fig. 2c), realizing 2-fold improvement

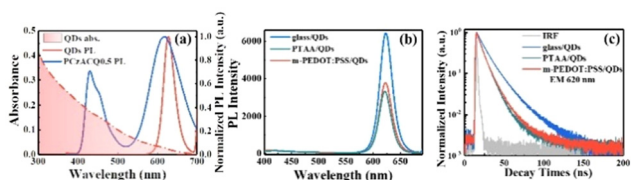


Fig. 1 (a) PL spectra of QD and PCzAQCO.5 films, and UV-vis absorption of QD film on glass substrates, respectively. (b) Steady PL spectra and (c) transient PL decay curves of the QD films on different substrates.

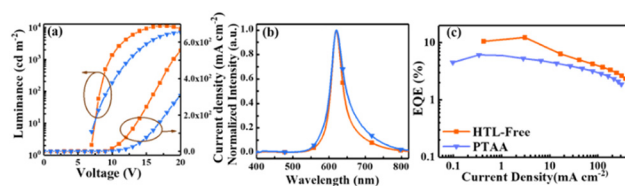


Fig. 2 (a) Luminance–voltage–current density curves of the devices with and without the HTL PTAA. (b) Normalized EL spectra of the devices recorded at a driving voltage of 10 V. (c) EQE–current density curves of QLEDs with PCzAQCO.5:QD as the EML.

through the HTL-free device strategy. These results demonstrated the high feasibility of this particular HTL-free strategy. However, the EL spectra shown in Fig. 2b imply that there was some residual emission from the host PCzAQCO.5, compared to the normalized PL spectrum shown in Fig. 1b. This sacrifices the color purity. The FWHMs are 36 and 45 nm for the HTL-free and PTAA based QLEDs, respectively.

In order to suppress the residual emission of PCzAQCO.5 and obtain a high color purity red QLED, we further introduced small molecular hosts, *i.e.*, 1,3-bis(carbazol-9-yl)benzene (mCP), bis(4-(9,9-dimethyl-9,10-dihydroacridine)phenyl)sulfone (DMAC-DPS), and bis-[3-(9,9-dimethyl-9,10-dihydroacridine)-phenyl]-sulfone (m-ACSO₂)²¹ to construct a ternary-blended EML and the TADF polymer PCzAQCO.5 was applied as a sensitizer. The schematic device structures are shown in Fig. S2 (ESI[†]).

The PL spectra of the hosts are compared in the inset of Fig. 3a. With the configuration ITO/m-PEDOT:PSS (50 nm)/host: (40 wt.%) PCzAQCO.5:(20 wt.%) QD (40 nm)/DPEPO (10 nm)/TmPyPB (50 nm)/LiQ (1 nm)/Al (100 nm), we fabricated three more devices to investigate the influence of the hosts on the EL performances of the HTL-free QLEDs. Although the devices employed the TADF host, *i.e.*, DMAC-DPS and m-ACSO₂, the current density and luminance were not significantly superior to those with the fluorescent host mCP. It can be easily found that the DMAC-DPS and mCP based QLEDs possessed similar current density from Fig. 3b. The EQE *versus* current density curves shown in Fig. 3c demonstrate the superiority of the fluorescence host mCP. Consistent with the result shown in Fig. 3b, the QLED with the TADF host m-ACSO₂ only obtained a maximum EQE of 5.3% which was much lower than those of the devices with mCP (17.7%) and DMAC-DPS (10.8%), respectively. The EL results are summarized in Table S2 (ESI[†]).

The overlapping between the UV-vis absorption spectrum of PCzAQCO.5 and the PL spectrum of mCP assures the efficient Förster energy transfer from mCP to PCzAQCO.5, which accounts for the high EQE. As shown in Fig. 3d, the normalized

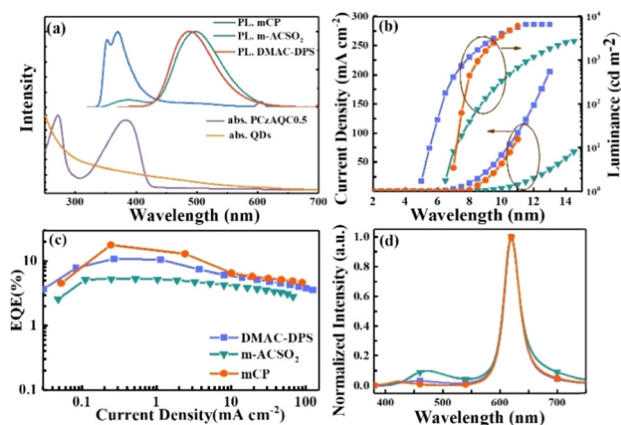


Fig. 3 (a) UV-vis absorption of QDs and PCzAQCO.5. Inset: PL spectra of mCP, DMAC-DPS, and m-ACSO₂, respectively. (b) Luminance-voltage-current density curves of the ternary-blended QLEDs with different hosts. (c) EQE-current density curves and (d) normalized EL spectra of the devices recorded at a driving voltage of 10 V.

EL spectra of the devices suggest QD emission in the range of 550–700 nm, although some residual emission from the hosts is also detectable, especially in the case of m-ACSO₂. This deteriorates the color purity which could be simply quantified using Eqn S1 (ESI[†]).^{22–24} Besides the highest EQE, a high color purity of 97.0% (see Table S2, ESI[†]) was realized for the device with mCP:PCzAQCO.5:QD as the EML. It is worth noting that the driving voltage required for the mCP based QLED was higher than of the device with DMAC-DPS (see Fig. 3b), partially due to the non-bipolar charge transport of mCP. We further optimized the thickness of the EML with mCP (40 *versus* 30 nm) and the doping concentration of QD (20 *versus* 30 wt.%). The EL performances are shown in Fig. S3 and Table S2 (ESI[†]). It is encouraging to observe that using a thinner EML (30 nm) led to a smaller FWHM and a reduced driving voltage (see Fig. S3a, ESI[†]), simultaneously. Moreover, the maximum EQE of 18.1% (see Fig. S3c, ESI[†]) was obtained when the QD concentration was fixed at 30 wt.%. The EL performances were sufficiently improved compared with those of the HTL-free device with only mCP:QD as the EML (Fig. S4, ESI[†]). These results confirmed that a high-color-purity and efficient QLED can be realized by using a ternary-blended host:TADF sensitizer:QD without any commonly used HTLs.

To further prove that the enhanced efficiency was attributed to the efficient Förster energy transfer within the ternary-blended system host:TADF sensitizer:QD, we measured the photophysical properties of the films consisting of mCP:PCzAQCO.5 (30 wt%), mCP:QD (30 wt%) and mCP:PCzAQCO.5(30 wt%):QDs (30 wt%), respectively. As shown in Fig. 4a, the steady PL spectrum of mCP:PCzAQCO.5 exhibited dual emission in the range of 400–500 nm and 550–700 nm, which originated from the polymer backbone and TADF moiety, respectively. Once QDs were blended, both the emission bands of PCzAQCO.5 in the mCP:PCzAQCO.5:QD film were efficiently quenched (see Fig. S3b, ESI[†]) and a narrow FWHM comparable to the intrinsic QD emission was obtained, indicating the efficient energy transfer from TADF sensitizers to QDs.

The transient PL decay curve of mCP:PCzAQCO.5(30 wt.%) films (see Fig. 4b) shows the apparent prompt (43.7 ns) and delayed (2.01 μs) decay components, originated from the TADF process of PCzAQCO.5 itself. Combined with the steady PL spectra shown in Fig. 4a, the narrow emission of the film with mCP:PCzAQCO.5:QDs at 550–700 nm was mainly attributed to QDs. Therefore, the prolonged lifetime observed at 620 nm of the ternary system mCP:PCzAQCO.5:QD (1.43 μs) can be

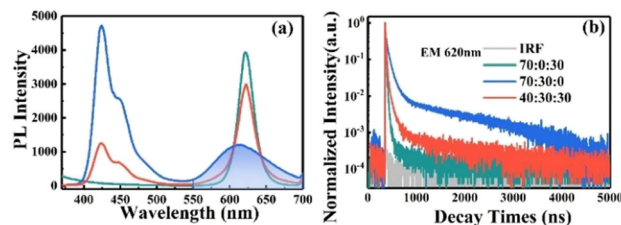


Fig. 4 (a) Steady and (b) transient PL decay curves of the films consisting of mCP:QD (green curve), mCP:PCzAQCO.5 (blue curve), and mCP:PCzAQCO.5:QD (red curve), respectively.

attributed to the delayed component of QDs emission resulting from the energy transfer from the up-converted excitons of PCzAQC0.5. In contrast, the transient PL lifetimes of the films with mCP:QD and mCP:PCzAQC0.5 were 75.3 ns and 2.01 μ s detected at 620 nm, respectively (see Table S3, ESI†). The PLQY of the ternary-blended film was slightly enhanced, compared with that of the binary-blended mCP:QD film, due to the utilization of triplet excitons in PCzAQC0.5 and subsequent efficient energy transfer to QDs. To further clarify the origin of the enhanced EL performances in the ternary-blend device without any HTLs, we determined the radiative and non-radiative recombination rate constants based on the PLQY and transient PL measurements.^{25,26} It is evident that, in terms of radiative recombination, the film with mCP:PCzAQC0.5:QD displayed an improvement factor of 2.2, compared with the binary-blended mCP:QD film. This indicates that efficient cascaded energy transfer occurred, leading to improved EL efficiency.

Conclusions

In summary, high-performance HTL-free red QLEDs with host:TADF sensitizer:QD ternary systems have been constructed for the first time. The TADF polymer sensitizer promotes Förster energy transfer from the host to QDs, and facilitates charge transport attributed to its bipolar nature. Achieving high-color-purity in doped QLEDs can be accomplished by managing the cascade energy transfer to remove the residual emission from the TADF sensitizer. The HTL-free structure enables high efficiencies and eases the device design of QLEDs. Unlike the common QLEDs with the metal oxide-based ETLs, the use of organic ETL design makes the devices easily reproducible and more compatible with large-area mass production. This work would provide a universal strategy to advance the development of the state-of-the-art QLEDs.

Author contributions

Conceptualization: G.X.; methodology: Y.G.; formal analysis: Y.G. and Q. X.; investigation: Y.G.; resources: Q.X. and G.X.; data curation: Y.G., Q.X., and G.X.; writing – original draft preparation: Y.G., Q.X. and G.X.; writing – review and editing: Y.G., Q.X. and G.X.; visualization: Y.H.; supervision: G.X.; project administration: G.X.; and funding acquisition: G.X. All authors have read and agreed to the published version of the manuscript.

Conflicts of interest

There are no conflicts to declare.

Acknowledgements

The authors acknowledge the funding support from the National Natural Science Foundation of China (no. 62175189).

This work was partially supported by the Open Fund of Key Laboratory for Preparation and Application of Ordered Structural Materials of Guangdong Province, Shantou University (no. KLPAOSM202003). G. X. acknowledges the funding support from the Program for Promoting Academic Collaboration and Senior Talent Fostering between China and Canada, Australia, New Zealand and Latin America (2021-109), and the joint China-Sweden Mobility programme (no. 52211530052). Prof. Yanxiang Cheng from the Changchun Institute of Applied Chemistry, CAS, China, is gratefully acknowledged for providing the TADF polymers used in this investigation.

Notes and references

- 1 X. Dai, Z. Zhang, Y. Jin, Y. Niu, H. Cao, X. Liang, L. Chen, J. Wang and X. Peng, Solution-processed, high-performance light-emitting diodes based on quantum dots, *Nature*, 2014, **515**, 96.
- 2 X. Peng, An essay on synthetic chemistry of colloidal nanocrystals, *Nano Res.*, 2010, **2**, 425.
- 3 S. Coe-Sullivan, Quantum dot developments, *Nat. Photonics*, 2009, **3**, 315.
- 4 X. Dai, Y. Deng, X. Peng and Y. Jin, Quantum-dot light-emitting Diodes for Large-Area Displays: Towards the Dawn of Commercialization, *Adv. Mater.*, 2017, **29**, 1607022.
- 5 Y. Shu, X. Lin, H. Qin, Z. Hu, Y. Jin and X. Peng, Quantum dots for display applications, *Angew. Chem., Int. Ed.*, 2020, **59**, 22312.
- 6 J. Song, O. Wang, H. Shen, Q. Lin, Z. Li, L. Wang, X. Zhang and L. Li, Over 30% External quantum efficiency light-emitting diodes by engineering quantum dot-assisted energy level match for hole transport layer, *Adv. Funct. Mater.*, 2019, **29**, 1808377.
- 7 J.-H. Kim, C.-Y. Han, K.-H. Lee, K.-S. An, W. Song, J. Kim, M. S. Oh, Y. R. Do and H. Yang, Performance improvement of quantum Dot-light-emitting diodes enabled by an alloyed ZnMgO nanoparticle electron transport layer, *Chem. Mater.*, 2014, **27**, 197.
- 8 Y. Zhao, C. Riemersma, F. Pietra, R. Koole, C. de Mello Donegá and A. Meijerink, High-temperature luminescence quenching of colloidal quantum dots, *ACS Nano*, 2012, **6**, 9058.
- 9 H. Chen, K. Ding, L. Fan, W. Liu, R. Zhang, S. Xiang, Q. Zhang and L. Wang, All-solution-processed quantum dot light emitting diodes based on double hole transport layers by hot spin-coating with highly efficient and low turn-on voltage, *ACS Appl. Mater. Interfaces*, 2018, **10**, 29076.
- 10 L. Qian, Y. Zheng, J. Xue and P. H. Holloway, Stable and efficient quantum-dot light-emitting diodes based on solution-processed multilayer structures, *Nat. Photonics*, 2011, **5**, 543.
- 11 H. Peng, Y. Jiang and S. Chen, Efficient vacuum-free-processed quantum dot light-emitting diodes with printable liquid metal cathodes, *Nanoscale*, 2016, **8**, 17765.

- 12 L. Xu, J. Li, B. Cai, J. Song, F. Zhang, T. Fang and H. Zeng, A bilateral interfacial passivation strategy promoting efficiency and stability of perovskite quantum dot light-emitting diodes, *Nat. Commun.*, 2020, **11**, 3902.
- 13 Y. Zou, M. Ban, W. Cui, Q. Huang, C. Wu, J. Liu, H. Wu, T. Song and B. Sun, A general solvent selection strategy for solution processed quantum dots targeting high performance light-emitting diode, *Adv. Funct. Mater.*, 2017, **27**, 1603325.
- 14 S. Wang, Y. Zhang, W. Chen, J. Wei, Y. Liu and Y. Wang, Achieving high power efficiency and low roll-off OLEDs based on energy transfer from thermally activated delayed excitons to fluorescent dopants, *Chem. Commun.*, 2015, **51**, 11972.
- 15 D. Zhang, X. Song, M. Cai and L. Duan, Blocking energy-loss pathways for ideal fluorescent organic light-emitting diodes with thermally activated delayed fluorescent sensitizers, *Adv. Mater.*, 2018, **30**, 1705250.
- 16 Y. Tao, K. Yuan, T. Chen, P. Xu, H. Li, R. Chen, C. Zheng, L. Zhang and W. Huang, Thermally activated delayed fluorescence materials towards the breakthrough of organoelectronics, *Adv. Mater.*, 2014, **26**, 7931.
- 17 M. Cai, D. Zhang and L. Duan, High performance thermally activated delayed fluorescence sensitized organic light-emitting diodes, *Chem. Rec.*, 2019, **19**, 1611.
- 18 Y. Xiang, G. Xie, M. Huang and C. Yang, Photophysics and electroluminescence of red quantum dots diluted in a thermally activated delayed fluorescence host, *J. Mater. Chem. C*, 2019, **7**, 13218.
- 19 T. Wang, K. Li, B. Yao, Y. Chen, H. Zhan, Z. Xie, G. Xie, X. Yi and Y. Cheng, Rigidity and polymerization amplified red thermally activated delayed fluorescence polymers for constructing red and single-emissive-layer white OLEDs, *Adv. Funct. Mater.*, 2020, **30**, 2002493.
- 20 Y. Xiang, G. Xie, Q. Li, L. Xue, Q. Xu, J. Zhu, Y. Tang, S. Gong, X. Yin and C. Yang, Feasible modification of PEDOT:PSS by poly(4-styrenesulfonic acid): a universal method to double the efficiencies for solution-processed organic light-emitting devices, *ACS Appl. Mater. Interfaces*, 2019, **11**, 29105.
- 21 K. Wu, Z. Wang, L. Zhan, C. Zhong, S. Gong, G. Xie and C. Yang, Realizing highly efficient solution-processed homojunction-like sky-blue OLEDs by using thermally activated delayed fluorescent emitters featuring an aggregation-induced emission property, *J. Phys. Chem. Lett.*, 2018, **9**, 1547.
- 22 X. Wang, Z. Zhao, Q. Wu, C. Wang, Q. Wang, L. Yanyan and Y. Wang, Structure, photoluminescence and abnormal thermal quenching behavior of Eu^{2+} -doped $\text{Na}_3\text{Sc}_2(\text{PO}_4)_3$: a novel blue-emitting phosphor for n-UV LEDs, *J. Mater. Chem. C*, 2016, **4**, 8795.
- 23 T. Zhao, H. Liu, M. E. Ziffer, A. Rajagopal, L. Zuo, D. S. Ginger, X. Li and A. K. Y. Jen, Realization of a highly oriented MAPbBr_3 Perovskite Thin Film via Ion Exchange for Ultrahigh Color Purity Green Light Emission, *ACS Energy Lett.*, 2018, **3**, 1662.
- 24 Q. Wang, G. Zhu, Y. Li and Y. Wang, Photoluminescent properties of Pr^{3+} activated Y_2WO_6 for light emitting diodes, *Opt. Mater.*, 2015, **42**, 385.
- 25 D. Chen, X. Cai, X.-L. Li, Z. He, C. Cai, D. Chen and S.-J. Su, Efficient solution-processed red all-fluorescent organic light-emitting diodes employing thermally activated delayed fluorescence materials as assistant hosts: molecular design strategy and exciton dynamic analysis, *J. Mater. Chem. C*, 2017, **5**, 5223.
- 26 K. Goushi, K. Yoshida, K. Sato and C. Adachi, Organic light-emitting diodes employing efficient reverse intersystem crossing for triplet-to-singlet state conversion, *Nat. Photonics*, 2012, **6**, 253.